Journal of Materials Chemistry A

ARTICLE

Highly permeable thermally rearranged polymer composite membranes with a graphene oxide scaffold for gas separation

Received 00th January 20xx,
Accepted 00th January 20xx

DOI: 10.1039/x0xx00000x

www.rsc.org/

Seungju Kim,[a] Jue Hou,[a] Yuqi Wang,[a] Ranwen Ou,[a] George P. Simon,[b] Jong Geun Seong,[c] Young Moo Lee,[c] and Huanting Wang*[a]

Thermally rearranged (TR) polymers are an important class of microporous polymers with remarkable gas transport performance, particularly suitable for CO_2 permeation and separation over large gas molecules. The fabrication of TR polymers into ultrathin membranes is highly desirable for practical application, but it is very challenging. In this work, a 2D scaffold of graphene oxide (GO) nanosheets was formed inside a TR polymer to assist the fabrication of a defect-free and ultrathin (less than 40 nm) selective layer of thermally rearranged polybenzoxazole-co-imide (TR-PBOI) membranes for energy-efficient CO_2 separation. The GO scaffold inside the polymer phase not only enabled the formation of the ultrathin selective layer of TR-PBOI, but also provided mechanical robustness. The resulting membrane showed remarkable gas permeance, while maintaining gas selectivity of the pristine polymer. In particular, it had a CO_2 permeance of 1784 GPU and a CO_2/CH_4 selectivity of 32; whereas the freestanding TR-PBOI membrane only exhibited a CO_2 permeance of 3.7 GPU with a CO_2/CH_4 selectivity of 35. In other words, rGO-PBOI (TR-PBOI with reduced GO) membrane has 482 times CO_2 permeance of TR-PBOI freestanding membrane at a similar CO_2/CH_4 selectivity.

Introduction

Membrane gas separation has been widely used in the industry, especially for CO_2 separation in natural gas sweetening and landfill gas upgrading due to its advantages such easy scale-up and relatively low energy consumption.[1] Since the traditional and currently dominant gas separation processes, such as thermally driven processes, are energy intensive and inefficient, the use of membranes for gas separation has been steadily growing over the last few decades.[1-4] More recently, CO_2 separation has attracted increasing interest for reducing the greenhouse gas emissions. A large number of organic and inorganic materials, such as microporous polymers, metal organic frameworks (MOFs) and carbons, have been studied for high performance membranes.[5-7] Ultra-permeable membranes with acceptable gas selectivity for efficient and economic process are favourable than ultra-selective membranes with moderate gas permeability since CO_2 separation process usually deals with a large volume of feed stream, and product purity can be controlled by designing process.[8] However, membrane gas permeability is the intrinsic property of materials, and highly permeable membrane presents low gas selectivity due to its trade-off relationship between gas permeability and selectivity.[9] Among many methods studied, tailoring microporous structures of membranes has been shown to be effective in improving both gas permeability and selectivity.

Microporous polymers with sufficient rigidity, such as thermally rearranged (TR) polymers and polymers of intrinsic microporosity (PIMs), have high selectivity and extraordinary gas permeability, overcoming the current performance limits of gas separation membranes in terms of gas permeability.[10-13] TR polymers based on polybenzoxazoles (PBOs) exhibit outstanding transport properties, especially for CO_2 separation.[10-21] The solid-state thermal decarboxylation reaction of aromatic polyimides (PIs) with ortho-positioned hydroxyl groups, called thermal rearrangement, results in TR polymers with very rigid polymer structures and regular distribution of free volume after the TR process.[10] Various research efforts have been made to characterise TR polymers and address the major challenge of TR polymers in fragility and brittleness for gas separation applications by optimising thermal treatment protocols,[12] introducing various chemical structures[13-15] and polymerisation routes of precursor PIs,[16] fabricating industry-preferred membrane modules,[17, 18] and investigating gas transport property in industrial process conditions.[14, 19, 21] By incorporating PIs with flexible functional groups, the resulting polybenzoxazole-co-imide (TR-PBOI) showed improved tensile strength and elongation at break of TR polymers, leading to an effective synthesis route to TR-PBOI membranes with both mechanical strength and separation properties.[19, 20]

[a] Department of Chemical Engineering, Monash University, VIC 3800, Australia.
[b] Department of Materials Science and Engineering, Monash University, VIC 3800, Australia.
[c] Department of Energy Engineering, Hanyang University, Seoul, 04763, Korea.

†Electronic Supplementary Information (ESI) available: Chemical structures of the monomers, PI and TR-PBOI membranes; TGA curves of PI and GO-PI freestanding membranes; ATR-FTIR spectra and XRD curves of PIs and PBOIs; SEM images of the surface and cross section AAO substrate, GO-PI and rGO-PBOI membranes; gas permeability and permeance of TR-PBOI freestanding membranes, rGO-PBOI membranes; mixed gas permeance of rGO-PBOI membranes. See DOI: 10.1039/x0xx00000x

The fabrication of ultrathin membrane is required to enable the high productivity in a membrane process due to decreased gas transport resistance of the membrane layer. Although various membranes with high gas permeability and high selectivity have been reported, only traditional polymers such as PIs, polysulfone (PSf), or cellulose acetates (CA) have been employed to fabricate hollow-fibre or spiral-wound membrane modules. This is because large-scale fabrication of asymmetric or composite membranes, such as hollow fibre, flat sheet, and thin film composite (TFC) membranes, with an ultrathin selective layer is challenging.[5] TFC membranes comprising a thin selective layer on a porous supporting layer are highly advantageous in membrane fabrication. This is because a polymeric or inorganic supporting layer provides mechanical strength required for high-pressure operation and reduces the membrane cost, and a thin selective layer of an advanced membrane material enables fast and selective transport of target molecules with a minimal amount of materials for membrane fabrication. A selective layer is deposited on the porous substrate by using various methods including conventional coating, such as spin-coating, filtration or casting of precursor solution, direct interfacial polymerisation of monomers, or secondary growth of MOFs using the interfacial synthesis on the semi-permeable barrier.[22-25] However, the thickness has been limited to few hundred nanometres because when reducing a layer thickness less than 100 nm, a layer tends to be defective, which significantly decreases gas selectivity.[26] Polyamide (PA) composite membrane with a defect-free selective layer less than 50 nm have been developed by interfacial polymerization, but its application is only limited to liquid separation due to its low performance in gas separation.[24]

Recently, highly ordered nanochannels derived from few-layered graphene, graphene oxide (GO) or two-dimensional (2D) MOFs have provided unique molecular transport for membrane-based applications such as ion separation, nanofiltration, and gas separation.[25-28] The interlayered nanochannels between 2D nanosheets with an atomic-level thickness enable the fast and precise molecular transport as well as mechanical strength, making them suitable for membrane applications. GO nanosheets, as membrane materials, are covalently crosslinked with organic linkers or incorporated into crosslinked polymer network to enhance the selective transport of small molecules and reduce swelling behaviour of GO.[23, 29, 30] However, the application of GO as a 2D scaffold for fabrication of ultrathin nanocomposite membranes for gas separation has not been reported.

In this work, we report for the first time the fabrication of ultrathin TR-PBOI membranes for gas separation by using GO scaffolds to improve the processibility of TR-PBOI and reduced its thickness to less than 40 nm. The resulting membranes exhibit the similar gas selectivity to the pristine TR-PBOI membranes, but greatly enhanced gas permeance. This method is highly promising for processing other polymer materials into ultrathin selective TFC membranes to boost their gas permeance for practical gas separation applications.

Experimental

Materials: For GO synthesis, graphite powder, sodium nitrate ($NaNO_3$), and potassium permanganate ($KMnO_4$) were purchased from Sigma-Aldrich (St Louis, MO) and used without further purification. Hydrogen peroxide (H_2O_2), sulfuric acid (H_2SO_4), hydrochloric acid (HCl) were purchased from Ajax Finechem (Taren Point, Australia) and used without further purification. For polymer synthesis, 3,3'-dihydroxyl-4,4'-diaminobiphenyl (HAB) was purchased from Wakayama Seika Kogyo (Wakayama, Japan) and 2,4,6-trimethyl-m-phylenediamine (DAM) was obtained from Chemtec (China, purified by sublimation, twice and stored under argon). All diamines were dried in an oven at 40°C with vacuum, overnight prior to the synthesis. 4,4'-(hexafluoroisopropylidene) diphthalic anhydride (6FDA) was purchased from Daikin Industries (Osaka, Japan) and dried in a vacuum oven at 100°C overnight to prevent cleavage of anhydride functional groups. N-Methyl-2-pyrrolidinone (NMP), o-xylene, methanol, and tetrahydrofuran (THF) were purchased from Sigma-Aldrich, and used as received. Porous anodic aluminum oxide (AAO) discs with 100 nm pores and a diameter of 13 mm (WhatmanTM) were obtained from GE healthcare (Little Chalfont, UK) and used as support.

GO synthesis: GO was synthesized from graphite powder using a modified Hummers' method.[31] Concentrated sulfuric acid (60 ml) was added to a mixture of graphite powder (2.5 g) and sodium nitrate (1.25 g) in an ice bath, then stirred for 30 min. Potassium permanganate (7.5 g) was slowly added and stirred in the ice bath for 2 h, then the solution changed from black to dark green. The solution was stirred for 12 h and deionised (DI) water (135 ml) was added, then stirred for 12 h. After adding hydrogen peroxide solution (30 wt%, 25 ml) and DI water (800 ml) the solution was stirred for 2 h. The resulting solution included GO and unreacted graphite, then GO was purified by centrifuge at 8,000 rpm, then washed with hydrochloric acid (5 wt%, 500 ml). After dialysis for a week to remove acid in solution, the GO solution was centrifuged at 9,800 rpm for 30 min to remove residual graphite and obtained in 3.8 mg ml^{-1} in water.

Polymer synthesis: Precursor copolymer of poly(amic acid) (PAA) was prepared from 6FDA with HAB and DAM as monomers using our previously reported procedure.[32] In a three-neck round-bottomed flask, 10 mmol of each diamine, DAM (1.5022 g) and HAB (2.1624 g), was sequentially dissolved in 20 ml of NMP under a nitrogen atmosphere and cooled in an ice bath. 20 mmol of 6FDA (8.8848 g) and 20 ml of NMP were then added to the flask. The mixture was vigorously stirred for more than 12 h, then a yellowish PAA solution was obtained. After that, 40 ml of o-xylene was added to the mixture as an azeotropic agent to prepare polyimides (PIs). The solution was heated up to 180°C under reflux for at least 12 h. Dean-Stark trap was used for the reflux. The resultant viscous and dark-brownish solution was cooled at room temperature and precipitated into a mixture of methanol and water (2L, Vol:Vol=1:3). The fibrous polymer precipitate was filtered and washed, with the methanol/water mixture more than five times

to remove residue reactants. PI powders were then dried at 120°C in a vacuum oven before use.

Membrane fabrication: The precursor solution for spin-coating included PIs and GO in THF. First, GO aqueous solution was freeze dried and re-dispersed in THF by sonication for 4 h and PI powder was dissolved under magnetic stirring in the solution. The weight ratio of GO and PI in the precursor solution was set to 2.0/100 (GO/PI) and the weight of total solid (GO-PI) in THF was controlled from 1.0 to 5.0%, and then the weight ratio between GO and PI was varied in the range of 0.5/100 to 2.4/100 (GO/PI) to optimise the fabrication process. The resulting membranes were denoted as GO-PI-X for precursors and rGO-PBOI-X for TR polymers, where X represents the weight ratio of GO to PI (X/100). The AAO substrate was set on a spin coater (WS-650-23B, Laurell Technologies Corporation, PA, USA), 0.5 ml of the precursor solution was spin-coated for 30 seconds at a controlled spinning rate of between 700 to 2,500 rpm, and then the membrane was placed in a convection oven (Thermal fisher, Scoresby, Australia) at 70°C for 2 h to completely dry a residual solvent. For characterising thermal stability of PIs and GO-PIs, freestanding membranes with thickness of 50 µm were prepared by casting of the solution in THF (10 wt%) and drying at 70°C for 12 h under vacuum. The PI and GO-PI membranes were thermally converted to thermally rearranged polybenzoxazole-co-imide (TR-PBOI) and reduced graphene oxide and TR-PBOI (rGO-PBOI) membranes in a tubular furnace at 425°C for 30 min under argon atmosphere.

Characterization: The morphology of the membranes was investigated with a field emission scanning electron microscope (FE-SEM, Nova NanoSEM 450, FEI, Hillsboro, OR). The chemical structure was analysed by Attenuated total reflectance Fourier transform infrared spectroscopy (ATR-FTIR, Spectrum 100, Perkin Elmer, Waltham, MA). The crystalline structure was determined by using an X-ray diffraction technique (XRD, Miniflex 600 X-ray diffractometer, Rigaku, Japan). Thermal stability and thermal rearrangement conditions were characterised by Thermogravimetric analysis (TGA, Pyris STA6000, Perkin Elmer, Waltham, MA).

Gas permeation measurements: The single gas permeation properties were measured by constant-volume and various-pressure method, so-called the "time-lag method" at room temperature using an in-house built apparatus. The membranes were carefully measured for their area and thickness, and three membrane samples were prepared and tested to minimized experimental errors. For the five types of representative small gases including H_2, CO_2, O_2, N_2, and CH_4, the feed side was maintained at 760 mmHg and the permeate side was under vacuum conditions. During measurement, the pressure at the permeate side was increased from 0 to 2 mmHg and continuously recorded by a pressure transducer of MKS Seris 901 Transducer (Andover, MA) on computer. For the binary mixed gas separation, the flow rate of feed gas was fixed at 10 ml min^{-1} for each gas (1:1 mixture) and the flow rate of sweep gas was fixed at 50 ml min^{-1}. The gas composition was analyzed by a gas chromatography using SRI 8610C (Torrance, CA) with argon as a carrier and a sweep gas at room temperature. We have previously reported the details of the experimental setup.[33] The gas permeability coefficients were obtained from the pressure increase ratio at the permeate side as a function of operation time and calculated by the following equation:

$$\boldsymbol{P} = \left(\frac{\boldsymbol{VT_0 l}}{\boldsymbol{p_0 T \Delta p A}}\right)\frac{\boldsymbol{dp}}{\boldsymbol{dt}} \quad (1)$$

where P (Barrer) is gas permeability, V (cm^3) is the volume at permeate side, l (cm) is the membrane thickness, p (cmHg) is the pressure difference between the feed and the permeate, T (K) is the measurement temperature, A (cm^2) is the effective membrane area, p_0 and T_0 are the standard pressure and temperature, and dp/dt is the rate of the pressure increase. The ideal selectivity for single gas permeation and the separation factor for mixed gas permeation were defined as the ratio of the gas permeability of two gas components.

Results and discussion

Ultrathin TR-PBOI membrane was fabricated by formation of a thin layer of precursor GO and PI (GO-PI) on a porous inorganic substrate and subsequent thermal rearrangement, as schematically illustrated in **Fig. 1**. The PI in copolymer structure with flexible and rigid functional groups was chosen because its TR-PBOI membrane exhibited high gas permeability and mechanical property. The PI was prepared using a conventional condensation reaction for poly(amic acid) synthesis and the following azeotropic imidization as their chemical structures were described in Fig. S1.[19] The GO was synthesized from graphite powders by a modified Hummers' method.[31] For the fabrication of the composite membrane, the precursor solution containing PIs and GO in tetrahydrofuran (THF) was prepared and coated on an anodic aluminum oxide (AAO) substrate, and then the composite membrane of GO-PI was converted to reduced graphene oxide and TR-PBOI (rGO-PBOI) after the thermal rearrangement at 425°C for 30 min in an argon atmosphere. Thermal treatment at high temperature triggered decomposition of functional groups on GO and the GO became reduced.[34] Although there are no covalent bonds between PIs and GO, they are well mixed together in an organic solvent due to the low concentration used for spin-coating. Having hydroxyl groups on both GO and PIs also helped to improve uniformity of the membrane layer. Thermal rearrangement conditions were confirmed by thermogravimetric analysis (TGA) of freestanding PI and GO-PI membranes, investigating thermal rearrangement temperature described in Fig. S2 and duration time for 100% conversion from PI to TR-PBOI.

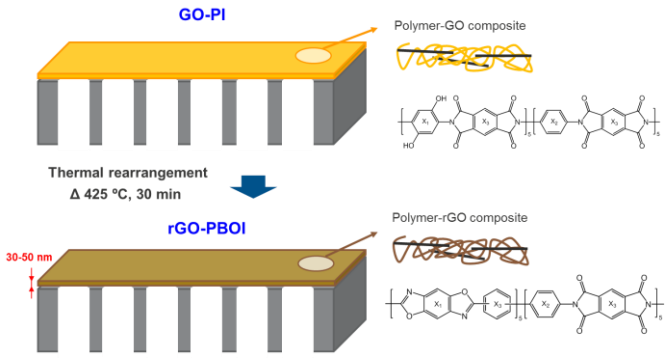

Fig. 1 Schematic of the polymer-GO composite membranes.

TR process is thermal reaction in solid state where non-porous PI is transferred to a microporous PBO structure. The completeness of the chemical conversion was confirmed by Attenuated total reflectance Fourier transform infrared spectroscopy (ATR-FTIR) spectra (Fig. S3) where a broad band of hydroxyl groups (3375 cm^{-1}) in GO-PI disappeared and a typical band of benzoxazoles (1558 cm^{-1}) appeared when converted to rGO-PBOI. The TR polymer was not influenced much by a small amount of GO in the precursor in terms of thermal stability and crystalline properties. As investigated by TGA and X-ray diffraction (XRD) in Fig. S2 and Fig. S4, TGA curves and XRD patterns of samples were almost identical. Therefore, the same TR protocol was used for GO-PI membranes. For GO nanosheets or GO-based membranes including GO-polymer composite membranes, a sharp peak at 8.5° was observed in XRD patterns, which represents the d-spacing of 1.04 nm between GO laminates.[35] However, no peak at 8.5° was observed for GO-PIs and rGO-PBOIs because well-dispersed GO nanosheets were mixed with polymers in solution and few layered GO nanosheets were stayed in the polymer phase as scaffolds. The broad XRD patterns for PI or PBOI were observed with the average d-spacing of 0.55 nm or 0.59 nm, respectively.

The morphology of the rGO-PBOI membrane on the AAO substrate was investigated by scanning electron microscopy (SEM). As shown in Fig. S5, small pores sized in average 100 nm on AAO were uniformly distributed. After coating of the GO-PI layer and subsequent thermal rearrangement, the rGO-PBOI layer was formed and no defect on the surface was found in the SEM image of rGO-PBOI-2.0 membranes (**Fig. 2a**). The GO-PI solutions in THF at low concentrations ranged from 1.0 to 5.0 wt% were used for spin-coating at 1000 rpm for 30 s to prepare a thin polymer layer. The choice of volatile solvent helped remove defects on the membrane and the low concentration helped significantly reduce the layer thickness. The effect of concentration on the membrane thickness was studied, as shown in SEM images in Fig. 2b-d. When the membrane was prepared from 5.0 wt% solution, the effective layer with about 85 nm thickness was observed (Fig. 2b). The thickness was significantly reduced to 35 nm when using a lower concentration of 1.5 wt% (Fig. 2d). The use of low concentration decreased amount of GO-PI for coating, the resulting membranes had a thinner membrane layer. However, the membrane prepared from 1.0 wt% solution was defected as the membrane layer was too thin and not fully covered with small cracks on the surface. The morphology of the GO-PI membrane did not change during thermal rearrangement, and the cross-sectional SEM images (Fig. S6) were almost identical between GO-PI and rGO-PBOI membranes.

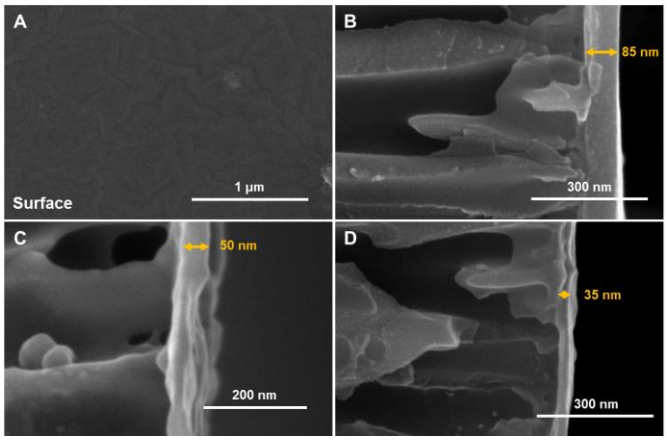

Fig. 2 SEM images of rGO-PBOI-2.0 membranes prepared from the solution in THF with a concentration of (a), (b) 5.0 wt%, (c) 2.0 wt%, and (d) 1.5 wt%.

The gas transport properties of the rGO-PBOI composite membranes were investigated by the constant-volume/variable-pressure method for single gas (H_2, CO_2, O_2, N_2 and CH_4) and the constant-pressure/variable-volume method for mixed gas (binary mixed gases of CO_2/N_2 and CO_2/CH_4 (1:1 mixture)) permeation measurement.[36-38] Table S1 presents the single gas permeability and permeance of TR-PBOI freestanding membrane, which possesses high H_2 and CO_2 permeabilities, 203 and 185 Barrers, respectively (1 Barrer = 10^{-10} cm^3(STP) cm/cm^2 s cmHg), and a high CO_2/CH_4 selectivity of 35. However, given a membrane thickness of 50 μm, gas permeance is calculated to be 4.1 and 3.7 GPU for H_2 and CO_2, respectively (1 GPU = 10^{-6} cm^3(STP)/cm^2 s cmHg = 3.35×10^{-10} mol/m^2 s Pa). Single gas permeances of rGO-PBOI membranes prepared under various conditions are shown in **Fig. 3**. Gas permeation unit (GPU) was used to present gas permeance, where membranes with a thinner layer exhibited higher gas permeance, although the same membrane material is used. The use of a low concentration of the precursor solution significantly reduced thickness of the membrane selective layer; and the resulting rGO-PBOI-2.0 membranes exhibited gradually increased gas permeance for all gases as shown in Fig. 3a. When the membrane was prepared from the 5.0 wt% solution, the rGO-PBOI-2.0 membrane had a CO_2 permeance of 380 GPU with a CO_2/CH_4 selectivity of 38. The CO_2 permeance was increased to 1149 GPU when the membrane was prepared from the 1.5 wt% solution, while its CO_2/CH_4 selectivity remained similar (39). It is clear that the thinner selective layer has the same quality (no defects) as the thicker one, demonstrating that GO plays a key role in the membrane formation. The effect of GO contents on gas permeance of rGO-PBOI membranes was investigated when the GO/PI weight ratio was varied from

0.5/100 to 2.4/100 at a fixed solution centration of 1.5 wt%. As shown in Fig. 3b, gas permeance of all gases decreased and gas selectivity for some gases slightly increased with increasing GO/PI ratio. Note that rGO-PBOI-0.5 membranes did not exhibit gas separation property, because GO ratio of 0.5/100 was too small and thus a defective layer was formed. rGO-PBOI-2.2 membranes exhibited CO_2 permeance of 872 GPU and CO_2/CH_4 selectivity of 43, and rGO-PBOI-1.0 membrane had CO_2 permeance of 1784 GPU and CO_2/CH_4 selectivity of 32.4. The permeance increase by reducing membrane thickness is remarkable as TR-PBOI freestanding membrane exhibits only 3.7 GPU for CO_2, whereas CO_2 permeance of rGO-PBOI membrane is 1784 GPU; in other words, rGO-PBOI membrane has 482 times CO_2 permeance of TR-PBOI freestanding membrane at a similar CO_2/CH_4 selectivity. Impermeable GO (or rGO) nanosheets dispersed in the polymer phase also increase gas permeation resistance, resulting in a decrease in gas permeance of rGO-PBOI membranes. However, when the amount of GO is too small, no continuous scaffolds are formed, leading to a defective TR layer, and lower gas selectivity. These high CO_2 permeance and CO_2/CH_4 selectivity are highly advantageous for practical separation processes such as natural gas treatment, since the high flux (high permeance) ensures high productivity. Moreover, high CO_2/N_2 selectivity of 17.7 for rGO-PBIO-1.0 membranes is very promising for post-combustion CO_2 capture process. The rGO-PBOI membranes were prepared by varying the spinning rate between 700 to 2,500 rpm in the spin-coating process to investigate the effect of spinning rate on gas permeance. The spinning rate can be a significant factor in determining the thickness and uniformity of polymer coating layers because of different centrifugal force to spread the coating solution.[39] As shown in Fig. 3c, gas permeance of rGO-PBOI-2.0 membrane slightly increased when a high spinning rate was used, but the difference was small. Since a volatile THF was used as a solvent, the spinning rate around 1,000 rpm was enough to form a thin and defect-free layer and the high spinning rate did not further affect the formation of rGO-PBOI membrane. Single gas permeance and ideal selectivity of rGO-PBOI membranes as a function of gas molecular kinetic diameter and a GO/PI ratio are shown in Fig. 3d and Table S2. TR polymers are capable of gas transport and separation based on precisely tuned pore sizes for CO_2 transport in the rigid polymer phases.[10] Therefore, the gas permeance gradually decreased with increasing kinetic diameter of gas molecule (i.e., larger gas molecules such as O_2, N_2, and CH_4).

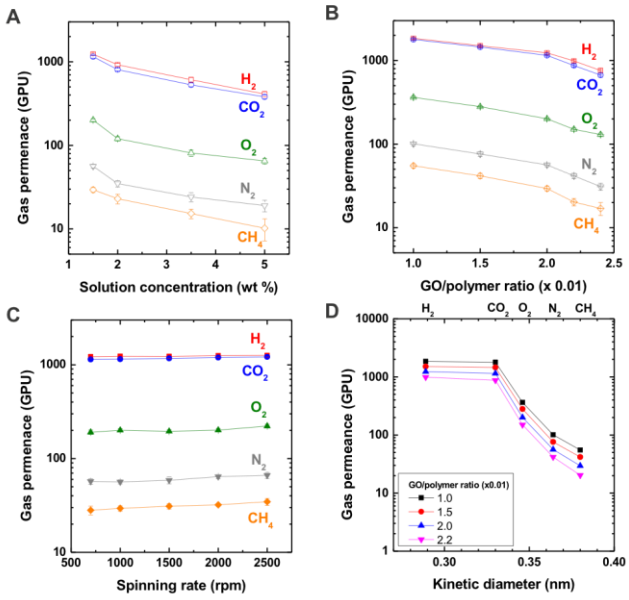

Fig. 3 Gas permeance of rGO-PBOI membranes as a function of (a) precursor solution concentration, (b) GO/PI ratio, (c) coating spinning rate, and (d) gas molecular kinetic diameter.

Equimolar binary gas mixtures of CO_2/CH_4 and CO_2/N_2 were used to evaluate CO_2 gas separation properties, and the results are summarized in Table S3. For polymer membranes, gas permeability and selectivity from mixed gas experiments often increase or decrease due to competitive gas permeation from gas mixture and plasticization effects for condensable gases.[21] In the case of rGO-PBOI membranes, the difference in CO_2 permeance between single and mixed gas measurements was quite small, less than 1% CO_2/CH_4 or CO_2/N_2 However, the selectivity for both CO_2/CH_4 and CO_2/N_2 slightly increased from 32.4 and 17.7 to 35.1 and 18.2, respectively. Gas transport through polymer phase is dominated by solution-diffusion mechanism where gas sorption and diffusion are involved in transport of gas molecules.[38] CO_2 as a condensable gas with high gas solubility in polymer phase effectively blocks transport of other gases during mixed gas permeation. Selectivity increases in CO_2 - CH_4 pair is higher than CO_2 - N_2 pair, meaning that transport of CH_4 is slowed down by CO_2 as CH_4 transport is dependent on both gas sorption and diffusion, whereas N_2 transport is dominated by gas diffusion.

CO_2 permeance and selectivity of rGO-PBOI membranes for CO_2/CH_4 and CO_2/N_2 are shown in **Fig. 4** with a comparison of highly CO_2 permeable membranes reported in the literature. Various membrane materials, such as TR-polymers,[17, 40] poly(butylene terephthalate)-poly(ethylene oxide) copolymer (PBT-PEG),[41] PIM nanocomposites,[42] and Pebax®-Ionic liquid composites (Pebax/IL),[43] have been prepared in a form of TFC and hollow fibre membrane. They presented either high gas permeance with low selectivity or high selectivity with low permeance because membranes with thin selective layer for high permeance tend to be defective. The relationship between gas permeability and selectivity is commonly used to evaluate gas transport properties of membrane materials.[9] This approach can also be applied for asymmetric membranes, such

as hollow fibre and TFC membranes with the relationship between gas permeance and selectivity. In Fig. 4, rGO-PBOI membranes demonstrated higher CO_2 permeance as compared with other high-performance membranes. Especially, rGO-PBOI membranes presented a remarkable CO_2/CH_4 separation performance since the gas permeation and separation properties of TR polymers are derived from its tuned cavity size and microporosity, where difference in kinetic diameters between CO_2 (3.3 Å) and CH_4 (3.8 Å) is larger than that of CO_2 and N_2 (3.64 Å).

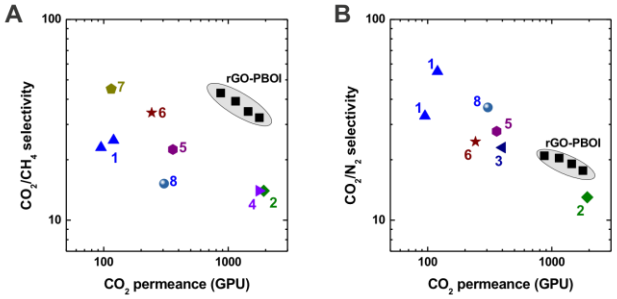

Fig. 4 Gas permeance and selectivity of rGO-PBOI membranes from single gas experiments with a comparison to literature data (1: GO,[28] 2: TR-PBO,[44] 3: Crosslinked TR-PBOI,[45] 4: PBT-PEG,[41] 5: PIM,[46] 6: PIM-Matrimid®,[46] 7: Crosslinked PI,[47] 8: Pebax/IL[48]).

Conclusions

In summary, we have developed a facile strategy for fabrication of ultrathin TR-PBOI membranes by spin-coating of the precursor solution of GO-PI on an inorganic substrate AAO and subsequent TR process at 425°C. GO was used as a scaffold in the TR polymer phase to form a defect-free membrane layer and thus reduce the selective layer thickness to about 35 nm. During TR heat treatment process, GO was also reduced to rGO, promoting interactions between two phases in the resulting rGO-PBOI membranes. The preparation parameters such as GO/polymer ratio in the precursor solution significantly influenced the gas transport performance of the resulting rGO-PBOI membrane. The rGO-PBOI membrane exhibited high CO_2 permeance of 1,784 GPU and CO_2/CH_4 selectivity of 32.4 and CO_2/N_2 selectivity of 17.7; such high CO_2 flux is highly advantageous for CO_2 separation processes such as natural gas purification or post-combustion CO_2 capture. This fabrication method and the membrane is highly reproducible and durable and can be further developed for large-scale membrane production. This strategy can be potentially used to process other membrane materials into ultrathin membranes with greatly enhanced molecular transport properties.

Conflicts of interest

There are no conflicts to declare.

Acknowledgements

The authors acknowledge the staff of Monash Centre for Electron Microscopy (MCEM) and The PerkinElmer Flagship Facility at Monash University for their technical assistance. This work was in part supported by the Australian Research Council (Project No. DP170102964).

Notes and references

1. P. Bernardo, E. Drioli and G. Golemme, *Ind. Eng. Chem. Res.*, 2009, **48**, 4638-4663.
2. X. Gao, X. Zou, H. Ma, S. Meng and G. Zhu, *Adv. Mater.*, 2014, **26**, 3644-3648.
3. S. Li, Z. Wang, X. Yu, J. Wang and S. Wang, *Adv. Mater.*, 2012, **24**, 3196-3200.
4. J. Zhang, J. A. Schott, Y. Li, W. Zhan, S. M. Mahurin, K. Nelson, X.-G. Sun, M. P. Paranthaman and S. Dai, *Adv. Mater.*, 2017, **29**, 1603797.
5. M. Galizia, W. S. Chi, Z. P. Smith, T. C. Merkel, R. W. Baker and B. D. Freeman, *Macromolecules*, 2017, **50**, 7809-7843.
6. Y. Liu, Y. Ban and W. Yang, *Adv. Mater.*, 2017, **29**, 1606949.
7. N. D. Boscher, M. Wang, A. Perrotta, K. Heinze, M. Creatore and K. K. Gleason, *Adv. Mater.*, 2016, **28**, 7479-7485.
8. T. C. Merkel, H. Lin, X. Wei and R. Baker, *J. Memb. Sci.*, 2010, **359**, 126-139.
9. L. M. Robeson, *J. Memb. Sci.*, 2008, **320**, 390-400.
10. S. Kim and Y. M. Lee, *Prog. Polym. Sci.*, 2015, **43**, 1-32.
11. H. B. Park, C. H. Jung, Y. M. Lee, A. J. Hill, S. J. Pas, S. T. Mudie, E. Van Wagner, B. D. Freeman and D. J. Cookson, *Science*, 2007, **318**, 254-258.
12. D. F. Sanders, Z. P. Smith, C. P. Ribeiro, R. Guo, J. E. McGrath, D. R. Paul and B. D. Freeman, *J. Memb. Sci.*, 2012, **409**, 232-241.
13. S. Li, H. J. Jo, S. H. Han, C. H. Park, S. Kim, P. M. Budd and Y. M. Lee, *J. Memb. Sci.*, 2013, **434**, 137-147.
14. K. T. Woo, G. Dong, J. Lee, J. S. Kim, Y. S. Do, W. H. Lee, H. S. Lee and Y. M. Lee, *J. Memb. Sci.*, 2016, **510**, 472-480.
15. Q. Liu, D. R. Paul and B. D. Freeman, *Polymer*, 2016, **82**, 378-391.
16. S. H. Han, N. Misdan, S. Kim, C. M. Doherty, A. J. Hill and Y. M. Lee, *Macromolecules*, 2010, **43**, 7657-7667.
17. S. Kim, S. H. Han and Y. M. Lee, *J. Memb. Sci.*, 2012, **403**, 169-178.
18. K. T. Woo, J. Lee, G. Dong, J. S. Kim, Y. S. Do, H. J. Jo and Y. M. Lee, *J. Memb. Sci.*, 2016, **498**, 125-134.
19. M. Cersosimo, A. Brunetti, E. Drioli, F. Fiorino, G. Dong, K. T. Woo, J. Lee, Y. M. Lee and G. Barbieri, *J. Memb. Sci.*, 2015, **492**, 257-262.
20. Y. Zhuang, J. G. Seong, W. H. Lee, Y. S. Do, M. J. Lee, G. Wang, M. D. Guiver and Y. M. Lee, *Macromolecules*, 2015, **48**, 5286-5299.
21. K. L. Gleason, Z. P. Smith, Q. Liu, D. R. Paul and B. D. Freeman, *J. Memb. Sci.*, 2015, **475**, 204-214.
22. Y. Hu, J. Wei, Y. Liang, H. Zhang, X. Zhang, W. Shen and H. Wang, *Angew. Chem. Int. Ed.*, 2016, **55**, 2048-2052.
23. S. Kim, X. Lin, R. Ou, H. Liu, X. Zhang, G. P. Simon, C. D. Easton and H. Wang, *J. Mater. Chem. A*, 2017, **5**, 1533-1540.

24. S. Karan, Z. Jiang and A. G. Livingston, *Science*, 2015, **348**, 1347-1351.
25. H. Li, Z. Song, X. Zhang, Y. Huang, S. Li, Y. Mao, H. J. Ploehn, Y. Bao and M. Yu, *Science*, 2013, **342**, 95-98.
26. S. Kanehashi, S. Sato, K. Nagai, P. M. Budd, N. B. McKeown, D. Fritsch, Y. Yampolskii, V. Shantarovich, L. Starannikova and N. Belov, *Membrane gas separation*, Wiley, Chichester, West Sussex, 2010.
27. S. Wang, Y. Wu, N. Zhang, G. He, Q. Xin, X. Wu, H. Wu, X. Cao, M. D. Guiver and Z. Jiang, *Energy Environ. Sci.*, 2016, **9**, 3107-3112.
28. H. W. Kim, H. W. Yoon, S.-M. Yoon, B. M. Yoo, B. K. Ahn, Y. H. Cho, H. J. Shin, H. Yang, U. Paik and S. Kwon, *Science*, 2013, **342**, 91-95.
29. R. Kumar, K. Gopalakrishnan, I. Ahmad and C. Rao, *Adv. Funct. Mater.*, 2015, **25**, 5910-5917.
30. Z. Jia and Y. Wang, *J. Mater. Chem. A*, 2015, **3**, 4405-4412.
31. W. S. Hummers Jr and R. E. Offeman, *J. Am. Chem. Soc.*, 1958, **80**, 1339-1339.
32. H. J. Jo, C. Y. Soo, G. Dong, Y. S. Do, H. H. Wang, M. J. Lee, J. R. Quay, M. K. Murphy and Y. M. Lee, *Macromolecules*, 2015, **48**, 2194-2202.
33. L. He, D. Li, D. Dong, J. Yao, Y. Huang and H. Wang, *J. Appl. Polym. Sci.*, 2012, **124**, 3383-3391.
34. Y. Zhu, M. D. Stoller, W. Cai, A. Velamakanni, R. D. Piner, D. Chen and R. S. Ruoff, *ACS Nano*, 2010, **4**, 1227-1233.
35. D. C. Marcano, D. V. Kosynkin, J. M. Berlin, A. Sinitskii, Z. Sun, A. Slesarev, L. B. Alemany, W. Lu and J. M. Tour, 2010.
36. Q. Fu, J. Kim, P. A. Gurr, J. M. Scofield, S. E. Kentish and G. G. Qiao, *Energy Environ. Sci.*, 2016, **9**, 434-440.
37. A. Achari, S. S and M. Eswaramoorthy, *Energy Environ. Sci.*, 2016, **9**, 1224-1228.
38. S. Kim, J. G. Seong, Y. S. Do and Y. M. Lee, *J. Memb. Sci.*, 2015, **474**, 122-131.
39. P. Jiang and M. J. McFarland, *J. Am. Chem. Soc.*, 2004, **126**, 13778-13786.
40. J. H. Lee, J. Lee, H. J. Jo, J. G. Seong, J. S. Kim, W. H. Lee, J. Moon, D. Lee, W. J. Oh and J.-g. Yeo, *J. Memb. Sci.*, 2017.
41. W. Yave, A. Car, J. Wind and K.-V. Peinemann, *Nanotechnology*, 2010, **21**, 395301.
42. M. L. Jue, V. Breedveld and R. P. Lively, *J. Memb. Sci.*, 2017, **530**, 33-41.
43. W. Fam, J. Mansouri, H. Li and V. Chen, *J. Memb. Sci.*, 2017, **537**, 54-68.
44. S. Kim, S. H. Han and Y. M. Lee, *J. Membr. Sci.*, 2012, **403**, 169-178.
45. J. H. Lee, J. Lee, H. J. Jo, J. G. Seong, J. S. Kim, W. H. Lee, J. Moon, D. Lee, W. J. Oh and J.-g. Yeo, *J. Membr. Sci.*, 2017.
46. M. L. Jue, V. Breedveld and R. P. Lively, *J. Membr. Sci.*, 2017, **530**, 33-41.
47. G. Liu, N. Li, S. J. Miller, D. Kim, S. Yi, Y. Labreche and W. J. Koros, *Angew. Chem.*, 2016, **128**, 13958-13962.
48. W. Fam, J. Mansouri, H. Li and V. Chen, *J. Membr. Sci.*, 2017, **537**, 54-68.

Table of Contents

A 2D scaffold of graphene oxide (GO) nanosheets is formed inside a polymer to assist the fabrication of a defect-free and ultrathin (< 40 nm) selective layer of thermally rearranged polybenzoxazole-co-imide (TR-PBOI) membranes for energy-efficient CO_2 separation. The resulting rGO-PBOI membrane has 482 times CO_2 permeance of TR-PBOI freestanding membrane at a similar CO_2/CH_4 selectivity.

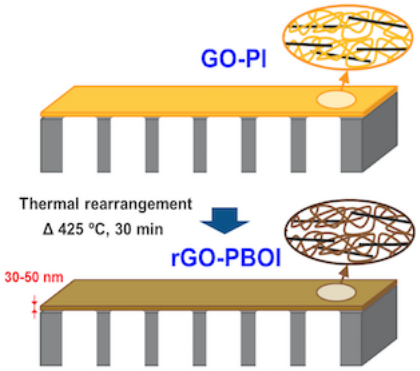

Supporting Information

Highly permeable thermally rearranged polymer composite membranes with a graphene oxide scaffold for gas separation

*Seungju Kim, Jue Hou, Yuqi Wang, Ranwen Ou, George P. Simon, Jong Geun Seong, Young Moo Lee, and Huanting Wang**

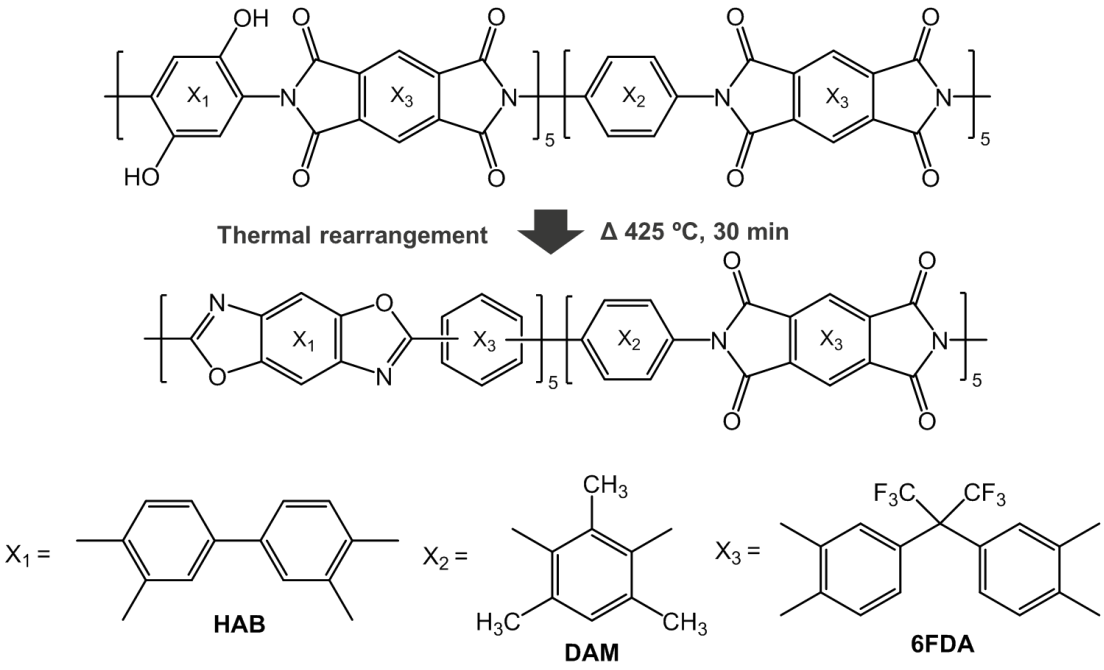

Fig. S1 Chemical structures of the monomers, PI and TR-PBOI membranes.

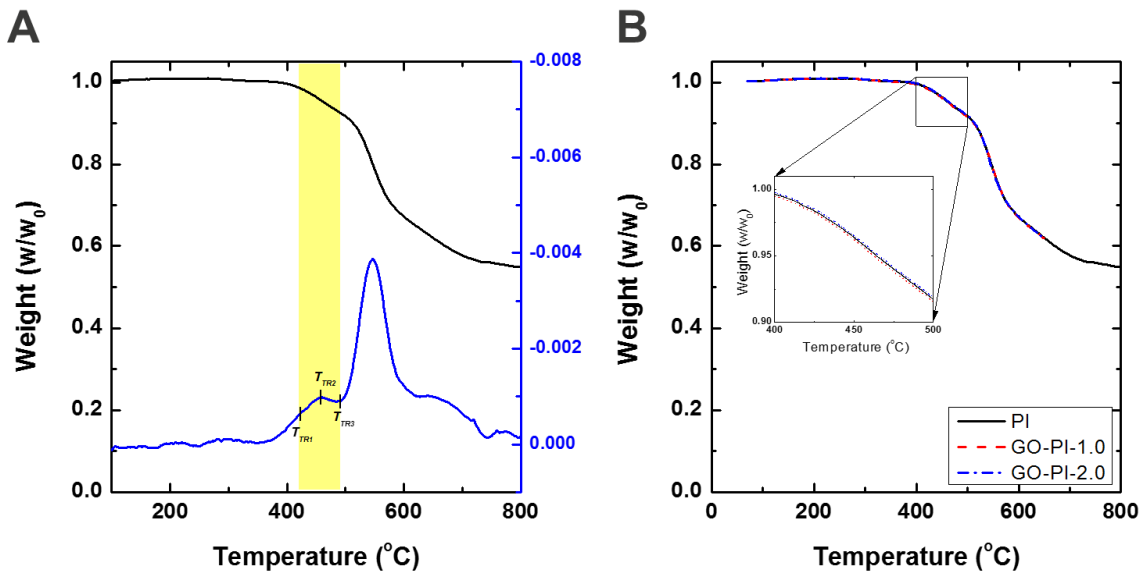

Fig. S2 Thermogravimetric analysis (TGA) curves of PI and GO-PI freestanding membranes.

The first weight loss between 420 ºC to 490 ºC represents thermal conversion from PI to PBOI. Thermal rearrangement temperatures (T_{TR1}, T_{TR1}, and T_{TR1}) were determined from its derivation curve and a duration time at 425 ºC was determined from its isotherm curve at 425 ºC by comparing to theoretical and experimental weight loss of thermal conversion.

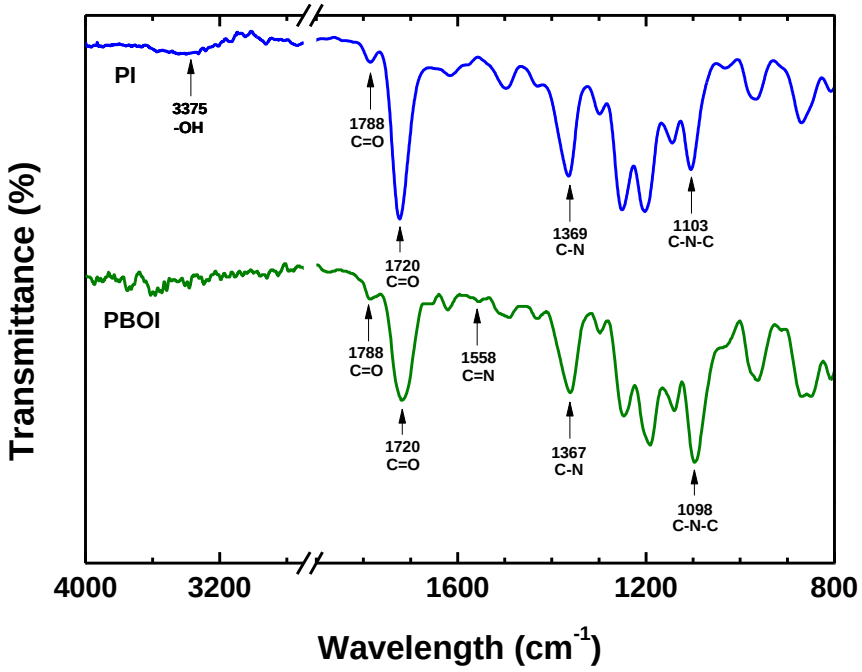

Fig. S3 Fourier transform infrared spectroscopy (ATR-FTIR) spectra of PIs and TR-PBOIs.

Typical bands of imide at 1788 cm^{-1}, 1720 cm^{-1}, 1369 cm^{-1}, and 1103 cm^{-1} were found in both PIs and PBOIs and a broad band of hydroxyl groups (3375 cm^{-1}) was only observed in PIs. Hydroxyl groups in PI and GO were disappeared during thermal rearrangement and a typical band of benzoxazoles (1558 cm^{-1}) was appeared.

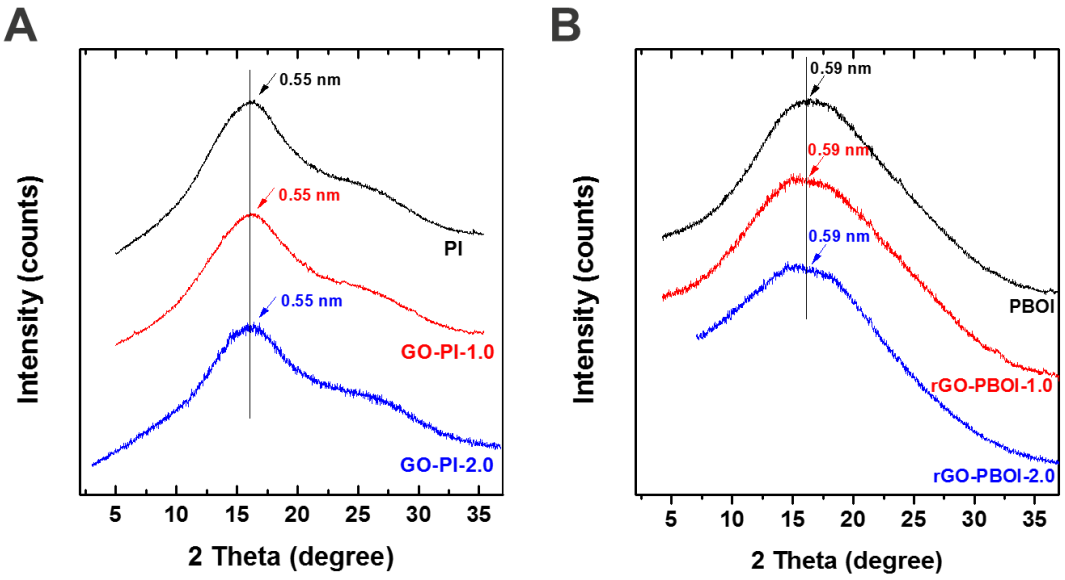

Fig. S4 X-ray diffraction (XRD) curves of PIs and TR-PBOIs.

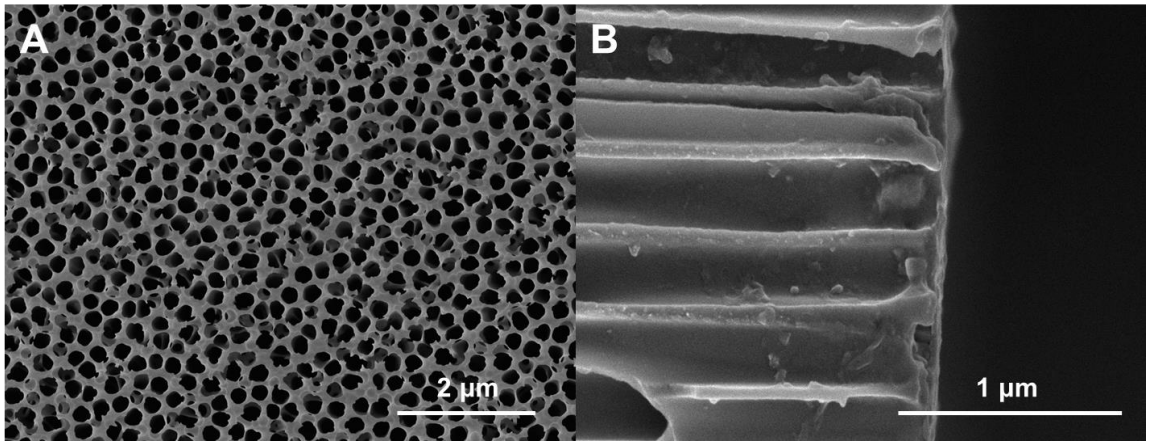

Fig. S5 Scanning electron microscope (SEM) images of AAO substrate (a) surface and (b) cross-section.

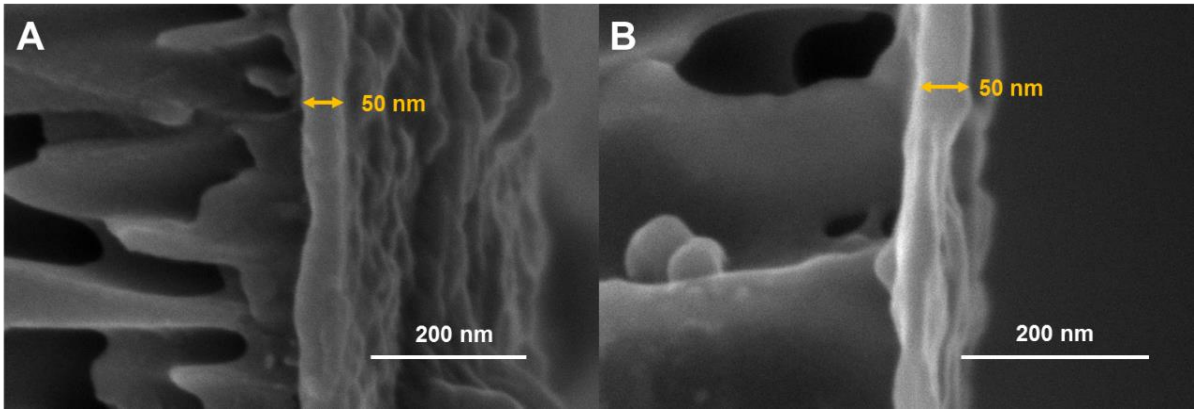

Fig. S6 Scanning electron microscope (SEM) images of (a) GO-PI-2.0 and (b) rGO-PBOI-2.0 prepared from 2.0 wt% solution in THF.

Table S1. Single gas permeability and permeance of TR-PBOI freestanding membranes.

	H_2	CO_2	O_2	N_2	CH_4	H_2/N_2	CO_2/N_2	O_2/N_2	CO_2/CH_4
Permeability (Barrer*)	203	185	32	7.5	5.3				
Permeance (GPU*)	4.1	3.7	0.64	0.15	0.11				
Ideal selectivity						27	26	4.2	35

*1 Barrer = 10^{-10} cm^3(STP) cm/cm^2 s cmHg = 3.35×10^{-16} mol m/m^2 s Pa
*1 GPU = 10^{-6} cm^3(STP)/cm^2 s cmHg = 3.35×10^{-10} mol/m^2 s Pa

Table S2. Single gas permeance of rGO-PBOI membranes.

	Gas permeance (GPU)					Ideal selectivity			
	H_2	CO_2	O_2	N_2	CH_4	H_2/N_2	CO_2/N_2	O_2/N_2	CO_2/CH_4
rGO-PBOI-1.0	1847	1784	363	101	55.1	18.3	17.7	3.6	32.4
rGO-PBOI-1.5	1505	1450	280	76	41.7	19.8	19.1	3.7	34.8
rGO-PBOI-2.0	1233	1149	201	56.4	29.4	21.3	20.4	3.6	39.1
rGO-PBOI-2.2	986	872	150	41.7	20.3	23.7	20.9	3.6	43.0
rGO-PBOI-2.4	761	673	125	30.7	15.1	24.8	21.9	4.1	44.6

Table S3. Mixed gas permeance of rGO-PBOI-1.0 membranes.

Gas permeance (GPU)				Separation factor	
CO_2 - CH_4 pair		CO_2 - N_2 pair			
CO_2	CH_4	CO_2	N_2	CO_2/CH_4	CO_2/N_2
1780	50.7	1785	98.1	35.1	18.2